



**Marian Klasztorny<sup>1\*</sup>, Daniel Nycz<sup>2</sup>**

<sup>1</sup> Military University of Technology, Faculty of Mechanical Engineering, Department of Mechanics & Applied Computer Science  
ul. gen. S. Kaliskiego 2, 00-908 Warsaw, Poland

<sup>2</sup> DES ART Sp. z o.o., Headquarters GDYNIA, Office SANOK, ul. Lipinskiego 113, 38-500 Sanok, Poland

\* Corresponding author. E-mail: m.klasztorny@gmail.com

Received (Otrzymano) 01.02.2013

## EFFECT OF CROSS-SECTION GEOMETRY ON LOAD CAPACITY OF SINGLE-WAVE COMPOSITE SEGMENT

The study examines a shell segment made of glass-polyester layered composites with fabric- or mat-reinforced layers. The segment is a single-wave, single-shell, and simply supported one, with a span, whose initial geometry and ply sequences were patterned after the cover segments of a selected rectangular tank in a sewage treatment plant in Germany. The aim of the study is multi-criteria quasi-optimization of the cross-section shape of the shell of the segment with flat flanges, with fixed, overall dimensions and ply sequences. The segment is subjected to a static three-point bending test with kinematic excitation. The optimization criteria are as follows: maximum load capacity of the segment, minimum weight of the segment, technological feasibility, and architectural effect. Numerical models of the segments with specified geometry of the cross-section (6 objects in total) were built using the Altair HyperMesh 11.0 system (finite element mesh) and MSC.Marc / Mentat 2010 (analysis set). The geometries were earlier prepared in the Generative Shape Design Catia v5r19 module. The numerical calculations (simulations) were performed using the MSC.Marc 2010 solver for non-linear analyses. The methodology for modeling and simulation of the composite shells, developed in the authors' previous papers, has been applied.

**Keywords:** polymer-matrix fibre-reinforced composite cover, single-wave rectangular segment, glass-polyester laminate, three-point bending test, cross-section, multi-criteria optimization

## WPŁYW GEOMETRII PRZEKRÓJU POPRZECZNEGO NA NOŚNOŚĆ JEDNOFALOWEGO SEGMENTU KOMPOZYTOWEGO

W pracy rozpatrzono segment powłokowy wykonany z kompozytów warstwowych poliestrowo-szkłanych mieszanych (warstwy wzmacnione tkaniną lub matą). Segment jest jednofałowy, jednopowłokowy, swobodnie podparty, o rozpiętości, geometrii wyjściowej i sekwenacji warstw wzorowanej na przekryciu wybranego zbiornika oczyszczalni ścieków. Celem pracy jest wielokryterialna quasi-optimizacja kształtu przekroju poprzecznego powłoki segmentu z płaskimi kolnierzami przy ustalonych wymiarach gabarytowych oraz sekwencjach warstw. Segment poddany jest próbie zginania statycznego trójpunktowego przy wymuszeniu kinematycznym. Kryteria optymalizacji są następujące: maksymalna nośność segmentu, minimalna masa segmentu, wykonalność pod względem technologicznym, efekt architektoniczny. Modele numeryczne segmentów o specyfikowanej geometrii przekroju poprzecznego (łącznie 6 obiektów) zbudowano przy użyciu systemu Altair HyperMesh 11.0 (siatka elementów skończonych) oraz systemu MSC.Marc / Mentat 2010 (opcje analizy). Geometrię segmentów przygotowano w module Generative Shape Design Catia v5r19. Obliczenia numeryczne (symulacje) wykonano za pomocą solwera analiz nie-liniowych w systemie MSC.Marc 2010. Zastosowano metodykę modelowania i symulacji powłok kompozytowych opracowaną w poprzednich pracach autorów. Metodyka quasi-optimizacji kształtu przekroju poprzecznego fali segmentu przekrycia kompozytowego, rozwinięta w niniejszej pracy, pozwala na relatywnie łatwe i szybkie wyznaczenie kształtu quasi-optymalnego. Jest to przekrój pośredni między półokręgiem a trójkątem równoramennym, któremu odpowiada wartość zmiennej decyzyjnej  $h = 0,5R$ . Proponowany przekrój quasi-optymalny jest estetyczny i atrakcyjny pod względem architektonicznym, łatwy do realizacji technologicznej, mający nośność prawie dwukrotnie wyższą niż nośność segmentu bazowego i masę mniejszą o około 17% w porównaniu z segmentem bazowym. Przekrój ten może być zastosowany również w przypadku segmentów wielofałowych wykorzystywanych w przekryciach kompozytowych zbiorników prostopadłościennych.

**Słowa kluczowe:** przekrycie kompozytowe, segment prostokątny jednofałowy, laminat poliestrowo-szkłany, test zginania trójpunktowego, przekrój poprzeczny, quasi-optymalizacja wielokryterialna

## INTRODUCTION

Polymer-matrix composite covers of rectangular tanks consist of single- or multi-wave segments joined together along horizontal flanges with rivetnut-bolt joints with structural clearances [1]. The segments are

single-shell or sandwich, anisotropic laminate structures, for which static calculation methods and design are in the research and development process [2-4]. The cross-sections of the individual waves of the cover

segments are generally of semi-circle or circle-segment shapes [5]. The European leader in the design of FRP composite roofs of civil engineering structures is C.F. Maier Europolst GmbH & Co. KG, a German company [1]. The company does not publish the methodology of static calculations or design of their composite roofs. The national research and design offices have been conducting research-design works in this area, with no special standards or engineering tables, e.g. [6].

The study concerns a shell segment made of mixed glass-polyester layered composites with fabric- or mat-reinforced layers. The segment is a single-wave, single-shell, and simply supported one, with a span, initial geometry and ply sequences patterned after the cover of a selected tank in the ZABA Boehringer Ingelheim sewage treatment plant, Germany [5]. The study focuses on a multi-criteria, quasi-optimization of the cross-section shape of the shell of the segment with flat flanges, assuming fixed overall dimensions and ply sequences. The segment is subjected to the static three-point bending test with kinematic excitation.

The optimization criteria are as follows: maximum load capacity of the segment, minimum weight of the segment, technological feasibility, and architectural effect. The methodology for modelling and simulation of composite shells, developed in Refs. [2-4], has been applied.

## STATE-OF-THE-ART

In FEM numerical modelling of laminates, composite layers are approximately modelled as linearly elastic-short materials. The most general homogenized model of layers reinforced with a balanced plain weave glass fabric or with a glass mat is a homogeneous orthotropic material with the orthotropy directions coinciding with the directions of the fibre alignments in the fabric. The 3-axis is perpendicular to the laminate plane. Each laminate layer is described by nine effective elasticity constants [7, 8]:

$E_i$  - Young's modulus in the  $i$  direction, where  $i = 1,2,3$ ,

$\nu_{ij}$  - Poisson's ratio in the  $ij$  plane, where  $ij = 12,23,31$ ,

$G_{ij}$  - shear modulus in the  $ij$  plane, where  $ij = 12,23,31$ ,

and by 18 effective strength constants [4, 5]:

$R_u, R_c$  - tensile strength and compressive strength in the  $i$  direction, where  $i = 1,2,3$ ,

$S_{ij}$  - shear strength in the  $ij$  plane, where  $ij = 12,23,31$ ,

$e_{it}, e_{ic}$  - ultimate normal strains in the  $i$  direction, regarding tension and compression, respectively, where  $i = 1,2,3$ ,

$g_{ij}$  - ultimate shear strain in the  $ij$  plane, where  $ij = 12,23,31$ .

These material constants are determined from the following standard strength tests:

1. static axial tension in the laminate plane,
2. static axial compression in the laminate plane,
3. static shear by unidirectional tension at angle  $\pm 45^\circ$  with respect to fibre directions,
4. static shear in the laminate plane with the Iosipescu method,
5. static interlayer shear.

The macro-mechanical models of layered composites are formulated in accordance to the appropriate lamination theory. Each layer is modelled as a separate homogeneous material. In the case of 2D models of layered shells, one can distinguish equivalent single-layer theories and discrete-layers theories [9-12]. In single-layer theory, a laminate is represented by a single layer of micro-mechanical properties estimated as the weighted average values of subsequent lamina properties. This model used in conjunction with the classic Kirchhoff - Love thin shell theory, is commonly known as the classical laminate theory (CLT) [8]. The von Kármán-type CLT model, useful for the analysis of geometrically non-linear laminate plates, was developed by Sun & Chin [12], while the model for thin shells was formulated by Saigal et al. [13].

Modelling the elastic behaviour of laminates with high accuracy requires taking into consideration the transverse shear deformation. Refined theories have been developed in [14] for plates and in [15] for shells. In these theories, a respective transverse shear correction coefficient is incorporated due to the assumption of constant shear deformation through the shell thickness. The mathematical modelling of laminates and sandwich laminate structures loaded statically was developed by Kreja [16] who analysed the geometric non-linearity of elastic shells in small, medium and large rotations, with a constant shell thickness. The strength of a polymer-matrix fibre-reinforced composite is associated with determining the effective limit stresses/strains in the complex stress/strain state, transmitted through the material, which cause total destruction of the material at any point. To assess the degree of effort of the laminate layer in a complex stress/strain state, respective strength theories should be used. To date, a number of strength hypotheses related to a single layer of laminate have been formulated including: the maximum stress criterion, maximum stain criterion, Tsai-Wu criterion, Hashin criterion, modified Hashin criterion and many other criteria formulated by Hill, Tsai, Hoffman, Chang etc. [7, 8, 17-19]. In the MSC.Marc system [18], the following layer-by-layer failure criteria are implemented: MAX Stress, MAX Strain, TSAI-WU, HOFFMAN, HILL, HASHIN, HASHIN-FABRIC, HASHIN-TAPE, and PUCK. In the simulation, one can select up to three hypotheses simultaneously. Based on the numerical and experimental identification and validation studies presented in Refs. [2-4], the following hypotheses have been selected: the HASHIN-FABRIC criterion for layers reinforced with balanced plain

weave fabric and the MAX Strain criterion for mat-reinforced layers. The HASHIN-FABRIC criterion is an extension of the Hashin failure criterion for orthogonal fabric materials. At each integration point, the MSC.Marc system calculates six failure indices in the stresses, of the values belonging to the interval  $[0, 1]$ , as defined in [18]. Analogically, for the MAX Strain criterion, six respective failure indices in the strains are calculated, as defined in Ref. [18].

## NUMERICAL MODELLING OF SEGMENT, THREE-POINT BENDING TEST SIMULATION AND QUASI-OPTIMIZATION

Let us consider a glass-polyester composite segment which is a single-wave, single-shell, simply supported one, with a span of  $l = 12.00$  m. The geometry and dimensions of the base segment which has a semicircular cross-section of the shell are mapped in Figure 1. Figure 2 shows the free support of the segment on rigid flat steel supports and loading of the segment during the three-point bending test using a rigid machine punch.

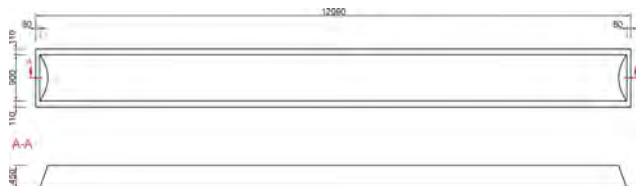


Fig. 1. Overall dimensions of base segment

Rys. 1. Wymiary gabarytowe segmentu bazowego

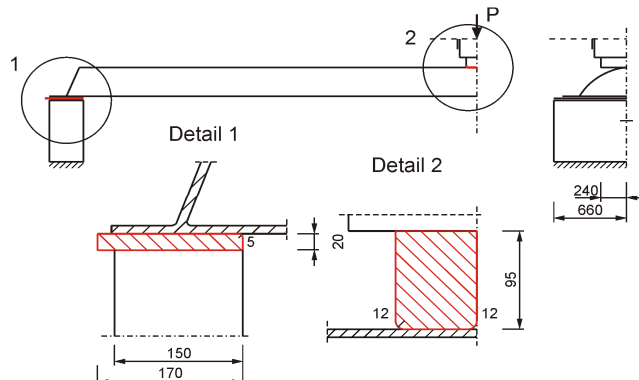


Fig. 2. Supporting and loading of single-wave composite segment in three-point bending test

Rys. 2. Podparcie i obciążenie segmentu kompozytowego jednofaładowego w próbie zginania trójpunktowego

The original segment, which is a component of the rectangular tank cover of the ZABA Boehringer Ingelheim waste-water plant, Germany [5], was made with Polimal 104T resin-based contact technology. The protective layers (gelcoat, topcoat) are 0.35 mm thick. The ply sequences and thicknesses of the mixed laminate structural layers are shown in Figure 3, where the following indications are introduced:

STR450 - a balanced plain weave E-glass fabric-reinforced layer, 450 g/m<sup>2</sup> weight (warp parallel to the axis of the segment),  
CSM300, CSM450 - an E-glass mat-reinforced layer, 300/450 g/m<sup>2</sup> weight.

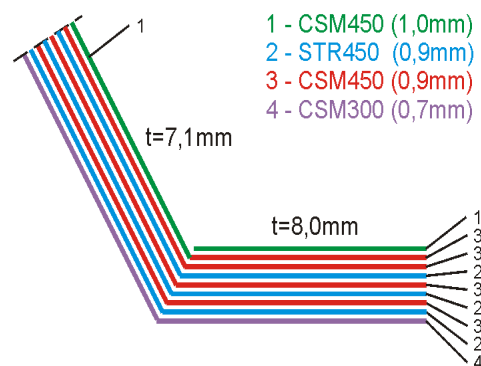


Fig. 3. Ply sequences in shell and flange of segment

Rys. 3. Sekwencje warstw powłoki i kolnierza segmentu

The material models of the laminae are linearly elastic-short orthotropic materials. The material constants were determined from identification experiments of the mechanical properties of uniform laminates at the temperature of 20°C [3]. Table 1 summarizes the material constants of uniform laminates reinforced with the fabric or mat. Subscripts t, c denote tension and compression, respectively. Some material constants were determined from the conditions imposed on orthotropic materials balanced in the 1,2-plane [7, 8, 19], i.e.

$$\begin{aligned}
 E_l &= \frac{1}{2}(E_{lt} + E_{lc}), \\
 E_{lt} &= E_{2t}, E_{lc} = E_{2c}, E_l = E_2, \\
 v_{12} &= v_{21}, v_{31} = v_{32}, v_{23} = v_{13}, \\
 G_{31} &= G_{32}, S_{31} = S_{32}, \\
 R_{lt} &= R_{2t}, R_{lc} = R_{2c}, \\
 e_{lt} &= e_{2t}, e_{lc} = e_{2c}, g_{31} = g_{32}, \\
 \frac{v_{ij}}{E_i} &= \frac{v_{ji}}{E_j}
 \end{aligned} \tag{1}$$

Based on the numerical and validation experimental studies developed in Refs. [2-4], the modelling and simulation of static processes in the mixed laminate shells use the options / values of modelling / simulation parameters given in Table 2.

In the 2D model of the composite segment, bilinear thick-shell finite elements (code 75) were used. This element is a 4-node 2D bilinear finite element of a thick shell type and has 3 translational and 3 rotational DOFs at each node. The membrane stresses are obtained from the displacement field, and the curvature is derived from the rotation field. Transverse shear strains are

calculated at the edge centres and interpolated to the integration points. The element can be used for analysis of the curved shells and complex plate structures. All the constitutive equations are available for this element [21].

TABLE 1. Material constants for mat- and fabric-reinforced layers

TABELA 1. Stale materiałowe warstw wzmocnionych matą i tkaniną

Material constant	CSM300, CSM450	STR450	Unit
$E_1$	8250	16550	MPa
$E_2$	8250	16550	MPa
$E_3$	4150	5000	MPa
$v_{12}$	0.390	0.155	-
$v_{23}$	0.235	0.234	-
$v_{31}$	0.118	0.0707	-
$G_{12}$	3200	2300	MPa
$G_{23}$	3100	2400	MPa
$G_{31}$	3100	2400	MPa
$R_{1t}$	95.7	269	MPa
$R_{1c}$	216	202	MPa
$R_{2t}$	95.7	269	MPa
$R_{2c}$	216	202	MPa
$R_{3t}$	70	70	MPa
$R_{3c}$	231	344	MPa
$S_{12}$	91	32.6	MPa
$S_{23}$	35.9	22.5	MPa
$S_{13}$	35.9	22.5	MPa
$e_{1t}$	0.021	0.021	-
$e_{1c}$	0.031	0.011	-
$e_{2t}$	0.021	0.021	-
$e_{2c}$	0.031	0.011	-
$e_{3t}$	0.017	0.020	-
$e_{3c}$	0.061	0.100	-
$g_{12}$	0.043	0.050	-
$g_{23}$	0.040	0.045	-
$g_{31}$	0.040	0.045	-
mass density $\rho$	$1.42 \cdot 10^{-9}$	$1.68 \cdot 10^{-9}$	t/mm <sup>3</sup>

Quasi-optimization of the cross-section shape of the shell segment of the semi-circular base cross-section was conducted in two stages. In the first stage, the semi-circular base outline was replaced by a semi-circle section and tangents, as shown in Figure 4. Numerical

modelling and simulation of the three-point bending test were performed in the base scenario and in two variants illustrated in Figure 4. In the second stage, the semi-circular base outline was replaced by a semi-circle section, as depicted in Figure 5. Numerical modelling and simulation of the three-point bending test were performed in the base scenario and in three variants according to Figure 5.

TABLE 2. Options/values of modelling / simulation parameters of static processes in mixed laminate shell structures

TABELA 2. Opcje/wartości parametrów modelowania / symulacji procesów statycznych konstrukcji powłokowych z laminatów mieszanych

Parameter in MSC.Marc system [20, 21]	Selected / determined option / value
Element Types	75 (Bilinear Thick-shell)
Element Dimensions	$\sim 20 \times 20$ mm
FAILURE	
Failure Criteria	Hashin-Fabric (fabric) Max Strain (mat) Max Strain
Failure	Progressive Failure
Stiffness Degradation Method	Gradual Selective
Residual Stiffness Factor	0.02
CONTACT	
Type	Touching (Node to Segment)
Separation Force	0.1
Distance Tolerance	0.25
Bias Factor	0.95
FRICTION	
Type	Coulomb
Numerical Model	Bilinear (Displacement)
Friction Force Tolerance	0.05
Slip Threshold	Automatic
ANALYSIS OPTIONS	
Max # Recycles	30
Min # Recycles	2
Iterative Procedure	Full Newton-Raphson
Convergence Testing	Residual and Displacement
Relative Force Tolerance	0.1
Relative Displacement Tolerance	0.1
Time Step	0.001
Nonlinear Procedure	Small Strain, Large Rotations Assumed Strain Large Rotation
Composite Integration Method	Full Layer Integration

The following symbols are adopted:

- cover\_00 - base segment in Figures 4 and 5 (for  $h = 0$ ),
- cover\_01 - segment shown in Figure 4 for  $h = 0.2R = 90$  mm,
- cover\_02 - segment shown in Figure 4 for  $h = 0.5R = 225$  mm,
- cover\_10 - segment shown in Figure 5 for  $h = 0.2R = 90$  mm,
- cover\_20 - segment shown in Figure 5 for  $h = 0.4R = 180$  mm,
- cover\_30 - segment shown in Figure 5 for  $h = 0.6R = 270$  mm.

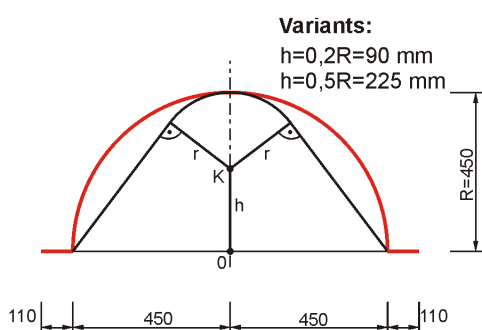


Fig. 4. First stage of quasi-optimization

Rys. 4. Pierwszy etap quasi-ptymalizacji

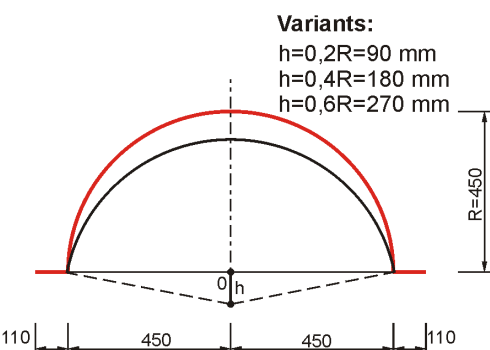


Fig. 5. Second stage of quasi-optimization

Rys. 5. Drugi etap quasi-ptymalizacji

Figure 6 shows the selected numerical model of the composite segment and depicts the planes of symmetry, the punch and the support. Because of bisymmetry, the model is limited to a quarter of the system. The base model (cover\_00) consists of more than 40 000 thick-shell finite elements. The individual finite elements of the model have assigned the orientation of the material properties in the *Material Properties / Orientations* card [18, 20]. The ply sequences are defined using the *Global Ply Number* option [20]. The supports were modelled as rigid surfaces rounded with a radius of 5 mm on the inside of the support. The loading punch was also modelled as a rigid body. The *Selective Gradual Degradation* model was applied [18].

Between the different components of the model (a quarter of the segment, the support and the punch) the *Node Segment - Touching* friction model was declared, based on the direct method [18]. In the contact model, the bilinear friction model was taken into account by declaring the friction coefficient  $\mu = 0.29$  and the limit stress  $\sigma_{gr} = 91$  MPa. The slip threshold was set by default.

The problem was solved using the full Newton-Raphson method in the FE code MSC.Marc, taking into account large displacements and small strains. The calculations took into consideration the force and displacement convergence criteria [18]. The tolerance of convergence in both cases was taken as 0.1 (the default). The calculation uses an adaptive increment in the loading time, assuming the values of the numerical parameters collected in Table 3.

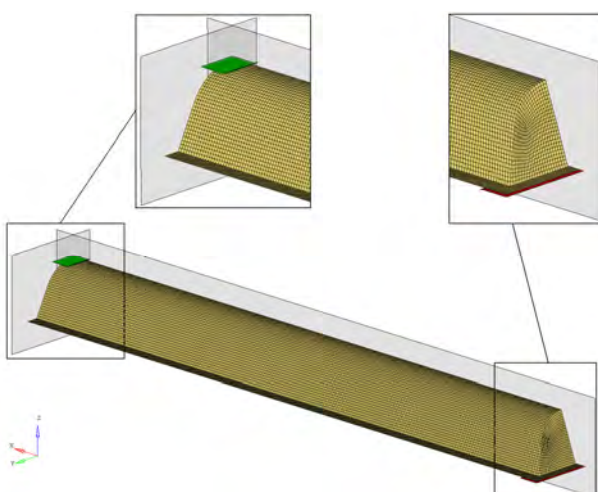


Fig. 6. Numerical model of composite segment in cover\_02 variant

Rys. 6. Model numeryczny segmentu kompozytowego w wariantie cover\_02

TABLE 3. Parameters of adaptive increment in loading time  
TABELA 3. Parametry zmiennego kroku przyrostowego w czasie obciążania

Parameter	Default	Assumed value
Initial Fraction of Loadcase Time	0.01	0.01
Minimum Fraction of Loadcase Time	$10^{-5}$	$10^{-4}$
Maximum Fraction of Loadcase Time	0.5	0.01
Desired # Recycles/Increment	5	5
Time Step Increase Factor	1.2	1.2

The numerical models of the segments were built using the *Altair HyperMesh 11.0* system (finite element mesh) and *MSC.Marc / Mentat 2010* (analysis set), and geometries prepared earlier in the *Generative Shape Design Catia v5r19* module. The numerical calculations were performed using the *MSC.Marc 2010* solver for non-linear analyses.

Each composite segment was divided into 4-node finite elements of a bilinear thick-shell element type, of an average size  $20 \times 20$  mm. The segment model was loaded in two phases. In the first phase (0 - 0.05 s), the linearly increasing gravity load was applied, while in the second phase (0.05 - 1 s), the linearly increasing kinematic loading was applied via vertical motion of the punch at a constant quasi-static speed. The nonlinear static equations of equilibrium were solved using the method of linearization of a non-linear curve in the incremental step with an iterative correction of the imbalance (full Newton-Raphson method).

Figure 7 shows the diagrams of the machine punch pressure force versus the testing machine traverse vertical displacement ( $F-s$ ), corresponding to the first stage of quasi-optimization. Figures 8-10 present the deformations of the cross-section at the midspan of the segment for the quasi-optimization variants, corresponding to the characteristic positions of the loading punch. Figure 11 presents the diagrams of the testing machine punch pressure force as a function of the testing machine traverse vertical displacement ( $F-s$ ), corresponding to the second stage of quasi-optimization.

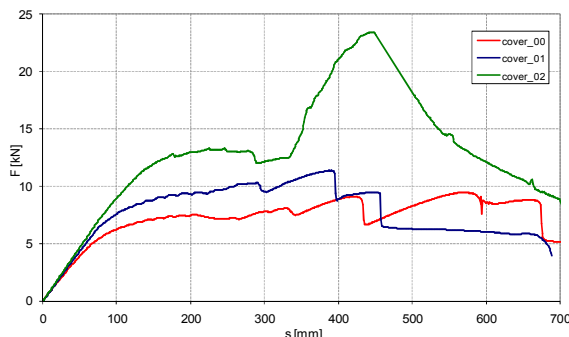


Fig. 7.  $F-s$  diagrams for first stage of quasi-optimization  
Rys. 7. Przebiegi  $F-s$  odpowiadające pierwszemu etapowi quasi-  
optymalizacji

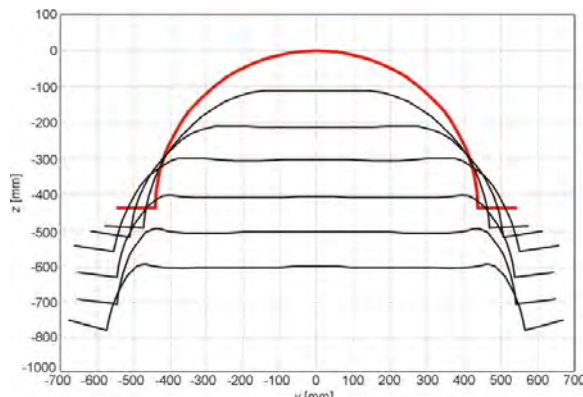


Fig. 8. Deformations of cross-section at midspan of cover\_00 segment for selected translations of punch  
Rys. 8. Deformacje środkowego przekroju poprzecznego segmentu cover\_00 odpowiadające wybranym przesunięciom stempla

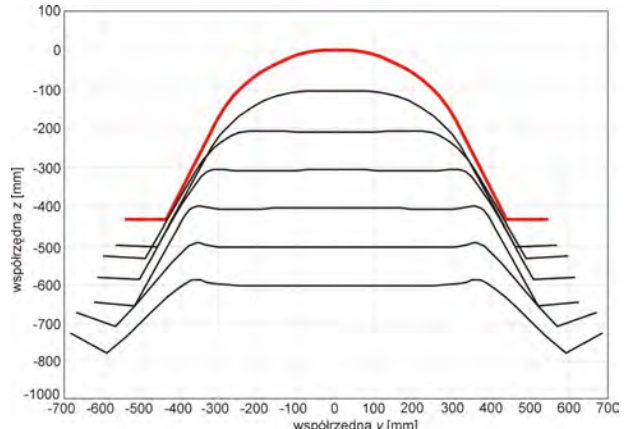


Fig. 9. Deformations of cross-section at midspan of cover\_01 segment for selected translations of punch  
Rys. 9. Deformacje środkowego przekroju poprzecznego segmentu cover\_01 odpowiadające wybranym przesunięciom stempla

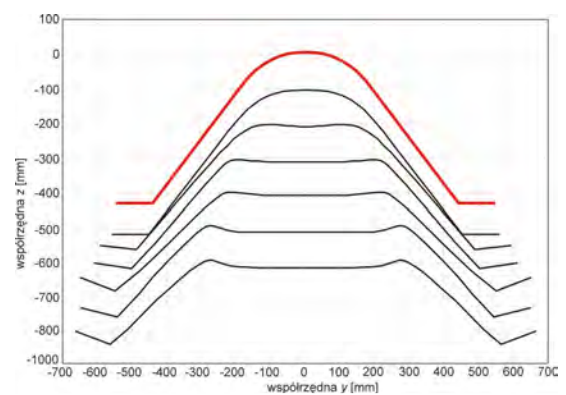


Fig. 10. Deformations of cross-section at midspan of cover\_02 segment for selected translations of punch  
Rys. 10. Deformacje środkowego przekroju poprzecznego segmentu cover\_02 odpowiadające wybranym przesunięciom stempla

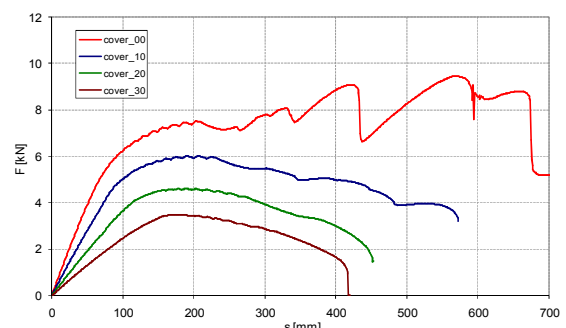


Fig. 11.  $F-s$  diagrams for second stage of quasi-optimization  
Rys. 11. Przebiegi  $F-s$  odpowiadające drugiemu etapowi quasi-optyma-  
lizacji

The first phase of quasi-optimization leads to the following conclusions:

- The  $s$  ranges of the linear elastic responses of the segments to the kinematic excitation (vertical motion of the machine punch) increase as parameter  $h$  rises, by 14% for  $h = 0.2R$  and 43% for  $h = 0.5R$ .
- The non-linear elastic responses of the segments are consistent in quality and also increase with the increase in parameter  $h$ .

- The responses above a nonlinear elastic zone correspond to the progressive destruction and local buckling of the segment shell. The inelastic responses are different for the searched values of parameter  $h$ .
- The load capacity of the segments, defined as the upper limit of the non-linear elastic response, is  $F = 6.5 \text{ kN}$  for  $h = 0$  (the base segment),  $F = 8.0 \text{ kN}$  for  $h = 0.2R$  (up 23%),  $F = 12.5 \text{ kN}$  for  $h = 0.5R$  (up 92%). The load capacity increases as parameter  $h$  grows. In the same conditions, the segment mass decreases by  $\sim 10\%$  for  $h = 0.2R$  and by  $\sim 17\%$  for  $h = 0.5R$ .
- For the maximum value  $h = R$ , the cross-section of the segment shell has the shape of an isosceles triangle. Architecturally, the semi-circle shape (in the base segment) is the most attractive, whereas a triangular shape is the least attractive.
- Taking into account the capacity, technological and architectural considerations, it was estimated that the intermediate segment with parameter  $h = 0.5R$  is the quasi-optimal segment.

The second phase of quasi-optimization leads to the following conclusions:

- The linear elastic zones extend themselves with the increase in parameter  $h$ . For  $h = 0.6R$ , this zone is twice as long as compared to the case of  $h = 0$  (base segment).
- The non-linear elastic response is varied in quality and quantity for the studied variants of the segment. The base segment provides the most stable solution. Together with the flattening of the shell, the critical load decreases.
- As expected, the load capacity of the segment, defined as the upper limit of the non-linear elastic response, decreases with flattening in the segment and is  $F = 6.5 \text{ kN}$  for  $h = 0$  (base segment),  $F = 5.7 \text{ kN}$  for  $h = 0.2R$  (down 12%),  $F = 4.5 \text{ kN}$  for  $h = 0.4R$  (down 31%),  $F = 3.5 \text{ kN}$  for  $h = 0.6R$  (down 46%). In the same conditions, the segment mass decreases.

## FINAL CONCLUSIONS

The method to quasi-optimize the shape of the cross-section of the wave of the segment of the composite cover, developed in the study, allows for relatively easy and rapid determination of the quasi-optimal shape. This is an intermediate cross-section, between a half-circle and an isosceles triangle, which corresponds to the value of the decision variable  $h = 0.5R$ . The proposed quasi-optimal cross-section is aesthetic and attractive in terms of design, and easy to manufacture. This cross-section can also be applied to the multi-wave segments commonly used in the composite covers of rectangular tanks.

The methodology of numerical modelling of layered glass-polyester composite shells, was developed and validated experimentally by the authors in previous papers [2-4]. The results obtained in this study are therefore fully reliable.

## Acknowledgements

*The study has been supported by the National Centre for Science, Poland, as a part of project No. N N506 1228 40, realized in the period 2011-2013. This support is gratefully acknowledged.*

## REFERENCES

- [1] Covering Systems - Technical Concept, C.F. Maier Europlast GmbH & Co KG, Königsbronn, Germany 2006.
- [2] Klasztorny M., Bondyra A., Romanowski R., Nycz D., Gotowicki P., Numerical modelling and simulation of RN-B composite joint tensile test and experimental validation, Composites Theory and Practice 2012, 12, 3, 198-204.
- [3] Nycz D., Bondyra A., Klasztorny M., Gotowicki P., Numerical modelling and simulation of the composite segment bending test and experimental validation, Composites Theory and Practice 2012, 12, 2, 126-131.
- [4] Klasztorny M., Bondyra A., Szurgott P., Nycz D., Numerical modelling of GFRP laminates with MSC.Marc system and experimental validation, Computational Material Science 2012, 64, 151-156.
- [5] Romanowski R., ROMA's experience in the design, construction and operation of composite roofs of tanks and channels [in Polish], Research report, ROMA Ltd., Grabowiec 2009.
- [6] Workshop design of composite cover of Oxygen Stability Chamber in Sewage Treatment Plant in Goleniów [in Polish], BP KE „ERPRO” Ltd., Rybnik 2011.
- [7] Daniel I.M., Ishai O., Engineering Mechanics of Composite Materials, Oxford Univ. Press, New York - Oxford 1994.
- [8] Jones R.M., Mechanics of Composite Materials, Taylor & Francis, London 1999.
- [9] Reddy J.N., On refined computational models of composite laminates, Int. J. for Num. Meth. in Eng. 1989, 27, 361-382.
- [10] Noor A.K., Burton W.S., Assessment of computational models for multilayered composite shells, Applied Mechanics Reviews 1990, 43, 67-97.
- [11] Shu X.P., A refined theory of laminated shells with higher-order transverse shear deformation, Int. J. Solids & Structures 1997, 34, 673-683.
- [12] Sun C.T., Chin H., Analysis of asymmetric composite laminates, AIAA Journal 1988, 26, 714-718.
- [13] Saigal S., Kapuria R.K., Yang T.Y., Geometrically nonlinear finite element analysis of imperfect laminated shells, J. Composite Materials 1986, 20, 197-214.
- [14] Dong S.B., Tso F.K.W., On a laminated orthotropic shell theory including transverse shear deformation, J. Applied Mechanics, Trans. ASME 1972, 39, 1091-1096.
- [15] Reissner E., Small bending and stretching of sandwich-type shells, NACA Report 1950, 975, 483-508.
- [16] Kreja I., Geometrically Non-Linear Analysis of Layered Composite Plates and Shells, Gdańsk Univ. Technol. Press, Gdańsk 2007.
- [17] Kurnik W., Tylikowski A., Mechanics of Laminated Elements [in Polish], Warsaw Univ. Technol. Press, Warsaw 1997.
- [18] Marc 2008 r1, Vol. A, Theory and User Information, MSC. Software Co., Santa Ana, CA, USA.
- [19] Tsai S.W., Composites Design, 4<sup>th</sup> edn., Think Composites, Dayton 1987.
- [20] Marc 2008 r1, User's Guide, MSC. Software Co., Santa Ana, CA, USA.
- [21] Marc 2008 r1, Vol. B, Element Library, MSC. Software Co., Santa Ana, CA, USA.

